Large-Scale Classification of Land Cover Using Retrospective Satellite Data

Article *in* Cybernetics and Systems Analysis · February 2016

DOI: 10.1007/s10559-016-9807-4

7 authors, including:


Mykola Lavreniuk
National Academy of Sciences of Ukraine


Sergii V. Skakun
University of Maryland, College Park


Andrey Yu. Shelestov
National Technical University of Ukraine Kiev…

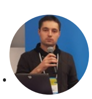
Bohdan Yailymov
Space Research Institute NAS Ukraine and S…

DOI 10.1007/s10559-016-9807-4
Cybernetics and Systems Analysis, Vol. 52, No. 1, January, 2016

LARGE-SCALE CLASSIFICATION OF LAND COVER USING RETROSPECTIVE SATELLITE DATA

M. S. Lavreniuk,[1†] **S. V. Skakun,**[2] **A. Ju. Shelestov,**[3] **B. Ya. Yalimov,**[1‡] **S. L. Yanchevskii,**[4] **D. Ju. Yaschuk,**[1††] **and A. M. Kosteckiy**[1†‡]

UDC 004.62, 004.67

Abstract. *Large-scale mapping of land cover is considered in the paper as a problem of automated processing of big geospatial data, which may contain various uncertainties. To solve it, we propose to use three different paradigms, namely, decomposition method, the method of active learning from the scope of intelligent computations, and method of satellite images reconstruction. Such an approach allows us to minimize the participation of experts in solving the problem. Within solving the problem of land cover classification we also investigated three different approaches of data fusion. The most efficient data fusion method is one that could be reduced to the problem of classification on the base of time-series images. Developed automated methodology was applied to land cover mapping and classification for the whole territory of Ukraine for 1990, 2000, and 2010 with a 30-meter spatial resolution.*

Keywords: *land cover classification, geospatial data, data fusion, satellite data, neural network, training and test samples.*

INTRODUCTION

Land cover maps or satellite data handling products are traditionally based on medium resolution pictures such as MODIS or SPOT VEGETATION [1]. Long-term archives of high-resolution satellite data, in particular, from Landsat satellite series and products of their preliminary processing, became available in recent years. This opens up new opportunities of large-scale retrospective mapping of higher (30-meter) resolution, which, in turn, allows tracing variations in land cover and land tenure and solving sustainable development problems [2–5].

However, large amount of high-resolution data not only opens up new possibilities but also generates new problems related to picture processing. Noteworthy is that methods of classification and formation of training sample, well-proven in handling one picture for a small area, appear unacceptable for large areas. The main problems are related to big data, small area covered by one picture, cloudiness, need to form a general map based on classification of pictures taken at different time, etc.

It is obvious that it is impossible to solve this problem by processing each picture separately by means of specialized software, for example ENVI. Therefore, it is necessary to minimize expert's role in problem solution by having automated all the stages of the solution, including the stage of satellite data classification and fusion of the obtained results. We will solve this problem in the paper.

---

[1]Institute of Space Research, National Academy of Sciences of Ukraine and State Space Agency of Ukraine, Kyiv, Ukraine, [†]*nick_93@ukr.net*; [‡]*yailymov@gmail.com*; [††]*yashchuk.dasha@gmail.com*; [†‡]*kosteckiyoleksandr@ gmail.com*. [2]"Integration Plus" Ltd., Kyiv, Ukraine, *serhiy.skakun@gmail.com*. [3]National University of Life and Environmental Sciences of Ukraine, Kyiv, Ukraine, *andrii.shelestov@gmail.com*. [4]National Center of Control and Testing of Spacecraft, Space Agency of Ukraine, Kyiv, Ukraine, *yanchevskiy@nkau.gov.ua*. Translated from Kibernetika i Sistemnyi Analiz, No. 1, January–February, 2016, pp. 137–149. Original article submitted April 9, 2015.

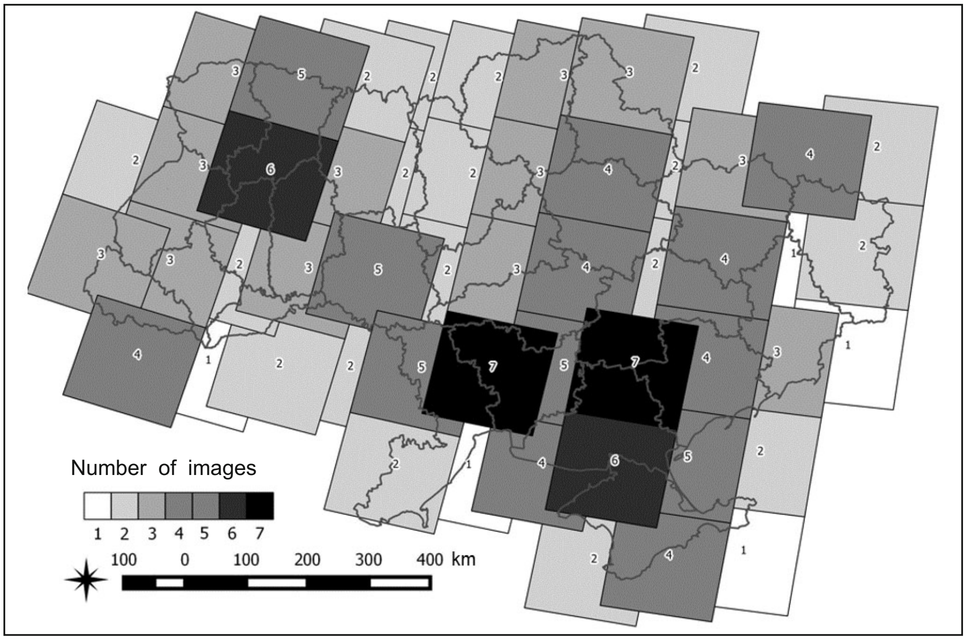

Fig. 1. Coverage of the territory of Ukraine by the scenes used
for classification on the basis of 2010 time series.

In solving the posed problem, intelligence systems are often applied to handle and use mass data and to improve the results obtained earlier on a regular basis [6]. They can be based on Grid and Sensor Web technologies [7–9] and on radar data [10].

GENERAL STATEMENT OF THE PROBLEM OF LARGE-SCALE LAND SURFACE CLASSIFICATION

The problem of classifying the territory of the whole country or a large region is a problem of big data handling and reduces to the following. Given unmarked long-term satellite images and reprsentative marked data obtained either by ground investigations or by photointerpretation, it is necessary to construct a classification map. The solution complexity of this problem is as follows:

- non-uniform cover of target territory by satellite images, which necessitates using different attributes for different regions. Figure 1 shows pictures of the territory of Ukraine taken by a satellite in 2010;
- the need to take into account local characteristics of the region under study (for example, the intensity and phases of development of agricultural crops may substantially vary depending on agroclimatic zones);
- data absence because of cloudiness and shades on optical images;
- uncertainty (inaccuracy) in marked data caused by their preparation on the basis of photointerpretation (subjectivity of expert's judgment).

To solve the problem posed in view of the above constraints, in the paper we propose an approach based on the use of three paradigms from different fields of computer sciences: the "divide and conquer" principle (from the theory of algorithms) [4], the active training method (from the machine training theory) [5], and image reconstruction method (from computer processing of digital images) [11].

To minimize the requirements to system's computing resources in solving big data handling problem, we propose to divide the territory of Ukraine into disjoint regions (according to the "divide and conquer" principle) and to solve classification problem for each of them. In the general case, this can be done in two ways:

- partition into same-size regions taking into account covering by satellite data [12];
- partition taking into account administrative districts.

The second way does not ensure equal squares of elementary domains; however, it has an advantage: it allows using independent information (for example, official statistical data, which are available to administrative districts of Ukraine) to validate the obtained maps. It is this approach that was used to create the map of the Earth surface classes in CORINE program, where each country investigated its own territory [13].

SOLUTION METHOD AND SATELLITE IMAGES CLASSIFICATION ALGORITHM

Consider the general approach to land surface classification for the whole territory of Ukraine on the basis of satellite data of high spatial resolution. Let P be the set of boundaries of polygons, G be a sample for some territory, consisting of pairs "polygon boundary" and class of land surface corresponding to this polygon, $G = \{(p, k) \mid p \in P, k = \overline{1, K}\}$, where k is land surface class and K is the total number of classes. It is expedient to store the sample in vector form to make it possible to use it in classification of satellite images of different resolution and size. Without loss of generality, we assume that in terrestrial measuring or in photointerpretation, the collected data are presented in the form of geometrical polygons. Denote the number of polygons in the sample (set potency) by $|G|$. Divide the sample into training and test parts, approximately in equal proportions, like in inductive approach. In this case,

$$G = G_{\text{train}} \cup G_{\text{test}}, \tag{1}$$

$$G_{\text{train}} \cap G_{\text{test}} = \varnothing. \tag{2}$$

As input data in the classification problem, we will consider long-term satellite images on which pixels hidden by clouds are reconstructed by the method from [11]. These images are used for each point of the selected territory to form the vector

$$\mathbf{x} = (x_1, x_2, \ldots x_n) \in R^n, \tag{3}$$

$$n = i \cdot c,$$

where i is the number of satellite images that cover the given point during a year and c is the number of spectral channels of satellite image.

Thus, the information arriving from spectral channels of satellite image can be used to generate the set of pixels of the sample, where each pixel belonging to the set of polygons G is associated with the respective class number

$$T(G) = \{(\mathbf{x}_i, k_i), i = \overline{1, N}\},$$

where N is the number of pixels in the sample. The potency and composition of this set depends on the set of polygons G. According to the partition of the set of polygons G (1), (2), the set of pixels T is also randomly divided into two independent subsets to train the classifier and to test it:

$$T = T_{\text{train}} \cup T_{\text{test}},$$

$$T_{\text{train}} \cap T_{\text{test}} = \varnothing.$$

The classifier $f(x)$ problem: for each input pixel (3), calculate the number of class k_{out} to which this pixel belongs.

In the present paper, as the classifier we will use multilayer perceptron (MLP), whose training and subsequent classification are performed pixel-by-pixel [14–16]. The choice of the specific model of the classifier is justified by the highest performance of the type of classifier in solving similar problems of classification of satellite images [17].

To train the classifier, the inverse error propagation method [18] is used. During classifier's training, adjustment of the weight factors of connections $w_{ij}^{(1)}$ between the input of neural network (3) and hidden neuron layer takes place, as well as $w_{jk}^{(2)}$ between the hidden layer and exit of neural network k_{out} so as to maximize the number of pixels for which the classifier correctly determines the value of reference class according to the training sample $k_{\text{out}} = k$. Figure 2 shows the flow chart of information processing in classifier's training with regard for the specific features of the problem.

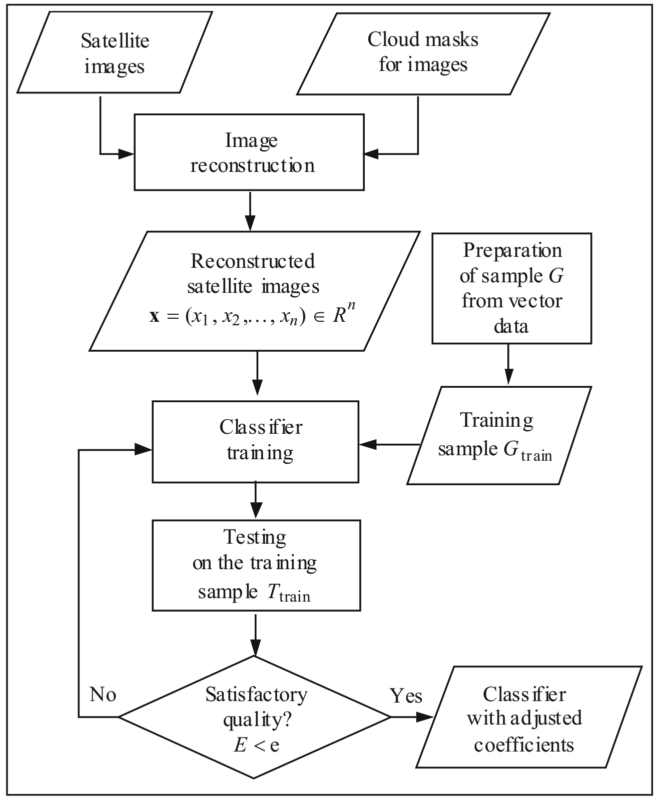

Fig. 2. The flow chart of training the classifier and adjustment of weight factors with the use of MLP.

After adjustment of classifier's parameters, pixel-by-pixel image classification is executed. As a result, we obtain classification map for all the pixels from necessary field. We will estimate its accuracy using an independent test sample and comparing with official statistical data.

To estimate the classification accuracy on an independent sample, we will use the following metrics.

Denote the part of pixels n_{ij} from the test sample that really belong to class i but are erroneously referred to class j, by n_{i+}:

$$n_{i+} = \sum_{j=1}^{K} n_{ij},$$

the part of pixels n_{ij} that actually belong to class j but are erroneously referred to class i by n_{+j}:

$$n_{+j} = \sum_{i=1}^{K} n_{ij}.$$

Then the total accuracy of the classification map is

$$OA = \sum_{k=1}^{K} n_{kk} / N.$$

Taking into account the notation, we can calculate errors of the first and second kind, i.e., accuracy of the "producer" PA and accuracy of the "user" UA, as well as the Kappa index K, which illustrates the level of classification "randomness" [19]:

$$PA = \frac{n_{jj}}{n_{+j}}, \quad UA = \frac{n_{ii}}{n_{i+}}, \qquad \mathrm{K} = \frac{N \cdot \sum_{i=1}^{K} n_{ii} - \sum_{i=1}^{K} n_{i+} \cdot n_{+i}}{N^2 - \sum_{i=1}^{K} n_{i+} \cdot n_{+i}}.$$

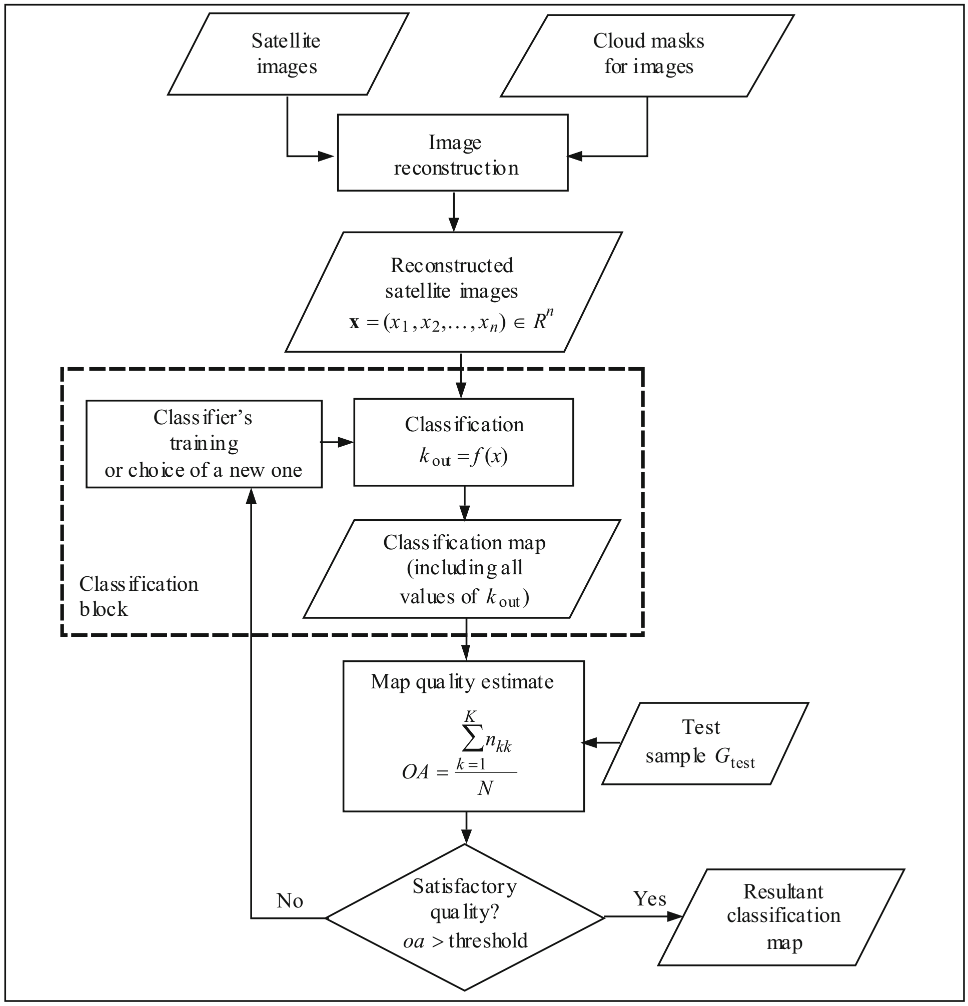

Fig. 3. Algorithm of active classification of satellite images.

Zero value of the Kappa index testifies that the result of classification agrees well with the sample in the same way as randomly assigned classes do.

If the quality (classification accuracy on an independent test sample) of the obtained map is satisfactory, it is accepted as the resultant map of classification. If the accuracy is unsatisfactory, additional training is performed or a new classifier is selected (active training).

Figure 3 presents generalized flow chart of classifier's operation with additional training (active training) in case of unsatisfactory accuracy of classification map on independent test sample. This approach, which includes reconstruction of noisy pixels and active training, ensures automatic construction of classification map for each selected part of the territory (administrative region of Ukraine). This is how the problem of classification of land cover for large areas is solved.

PRACTICAL IMPLEMENTATION OF THE PROPOSED APPROACH

The classification method described above was used to create retrospective land cover maps for the territory of Ukraine. The classification employed samples constructed according to the international nomenclature of classes LUCAS [20]. The constructed samples include polygons for six main classes (artificial objects), agricultural land, forest, uncultivated land, open ground, and water). For a detailed information about the generated samples and classes of land surface in 1990, 2000, and 2010, see Table 1.

TABLE 1

Class of Land Surface	Number of polygons in different years			Ratio of the number of polygons under study to the total number in different years (%)			Ratio of the area of polygons under study to the total area in different years (%)		
	2010	2000	1990	2010	2000	1990	2010	2000	1990
Artificial objects	29	14	38	0.22	0.12	0.32	0.04	0.03	0.07
Agricultural lands	6278	6000	5942	48.17	49.42	50.96	41.58	40.96	44.49
Forest	2338	2340	2332	17.94	19.27	20.00	17.28	18.00	20.83
Uncultivated land	2471	2084	1801	18.96	17.16	15.44	10.14	7.87	7.67
Open ground	315	180	156	2.42	1.48	1.34	1.06	1.47	0.96
Water	1601	1524	1392	12.29	12.55	11.94	29.90	31.67	25.98
Total	13032	12142	11661	100.00	100.00	100.00	100.00	100.00	100.00

Since training and test samples (Fig. 4) are generated based on photointerpretation, they do not contain absolutely reliable information because of the influence of subjective factor. Therefore, classification should be performed iteratively, by editing and filtering samples at each stage if needed. Let us formulate the generalized statement of classification problem as follows, taking into account sample filtration: modify iteratively the set G, so as to satisfy the following conditions:

$$E(T_{\text{train}}) \to \min,\ UA(G_{\text{test}}) \to \max,\ PA(G_{\text{test}}) \to \max, \tag{4}$$

$$|G| > g_{\text{critical}}, \tag{5}$$

where E is the function of neural network error under conditions (1), (2) and g_{critical} is the minimum number of polygons necessary for satisfactory training of the neural network [21, 22].

Thus, the sample is modified iteratively by eliminating errors (of the modification of polygons' boundaries and marking) and by adding new polygons until the classification quality becomes satisfactory. The number of selected polygons should satisy the conditions of a representativeness of classes in the domain under study and uniform cover of the area under study by polygons.

Construction of thematic map should be put in correspondence with current sample G and map of classification results and sample discrepancy should be generated. Since such discrepancies are caused by different reasons, first of all, it is necessary to ensure the fulfillment of condition (5), i.e., to provide uniform distribution of the training sample G_{train} over the area under study for all classes. For qualitative classification, it is also necessary that classes in training sample are distributed proportionally to the respective areas on the territory under study. Without regard for these requirements, though high classification accuracy will be obtained on test sample $UA(G_{\text{test}})$, $PA(G_{\text{test}})$, the resultant classification map will appear unsatisfactory.

Expert should analyze the results of classification of this field, sample G, and the time series of satellite images (3). The most popular reasons of the discrepancy between classification map and test sample are the following artifacts of the sample: overlapping of polygons pertaining to different classes; doubtful polygons (expert can hardly identify the class of a certain polygon); "mixed" polygons (containing inclusions of other classes such as small lakes or small groups of trees); atypical polygons (a polygon referred to some class substantially differs from other representatives of the same class), some other problems related to the quality of satellite images. To provide correct training of a neural network, doubtful polygons are deleted from the sample, incorrectly classified polygons should be correlated with the required class, atypical polygons are considered exceptions to the rules, i.e., outbursts, and are deleted. The iterative process is completed after identification of all noncomformities in the sample. The obtained classification map can be considered as the final result.

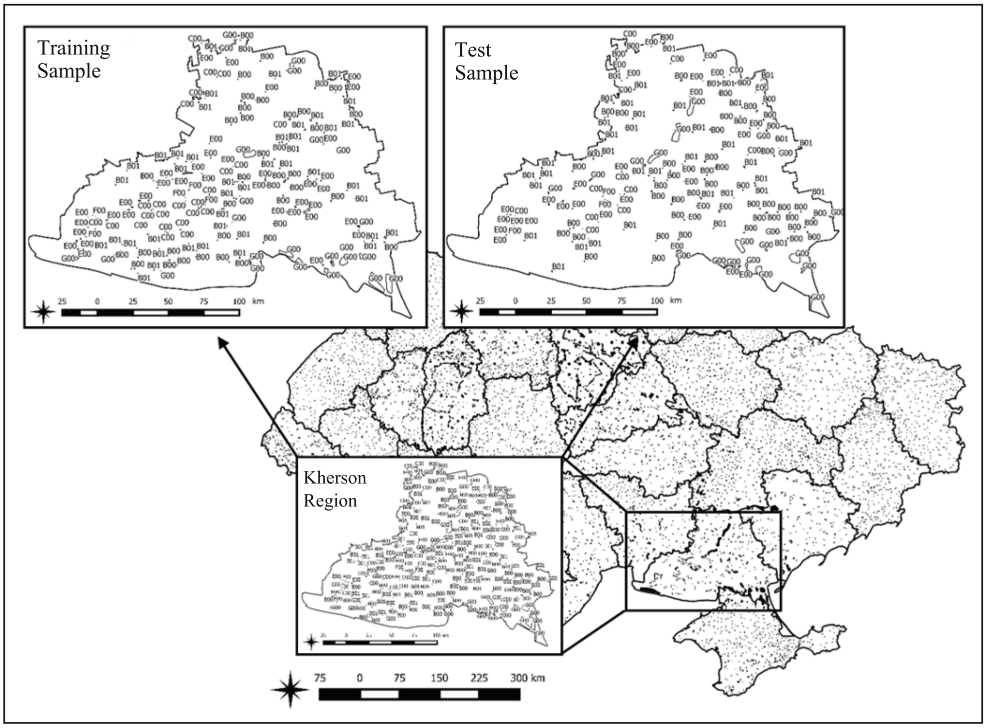

Fig. 4. Sample for the territory of Ukraine for 2010 with separate sample for the Kherson region.

DATA FUSION METHODS

Because of small area covered by one picture and presence of time series of pictures for each point (see Fig. 1), there is a problem of fusion of classification results and construction of the resultant map for a large territory. Two approaches to obtaining classification map are possible: (i) classification of each picture separately by the subsequent confluence of classification results into a general map for the given territory (fusion at decision making level); (ii) classification on the basis of the data from all the satellite images (time series of images) that cover the given point within a year (data fusion at pixel level) (3) [23, 24].

Within the framework of the first approach (fusion at decision making level) it is proposed to use two decision making methods. The first is to make a decision based on the probability of the membership of the given pixel to a certain class on each image covering the pixel. This approach to obtaining classification $\mathrm{Im}_{\mathrm{res}}(i, j)$ can be represented by the formula

$$\mathrm{Im}_{\mathrm{res}}(i, j) = \begin{cases} \mathrm{Im}_1(i, j), & P(\mathrm{Im}_1(i, j)) > P(\mathrm{Im}_2(i, j)), \\ \mathrm{Im}_2(i, j), & P(\mathrm{Im}_1(i, j) \le P(\mathrm{Im}_2(i, j)), \end{cases}$$

where $\mathrm{Im}_1(i, j)$ and $\mathrm{Im}_2(i, j)$ are the results of classification of pixel (i, j), $P(\cdot)$ is the event probability.

The second method of fusion at decision making level reduces to the following. Decision about the membership of the given pixel in some class $\mathrm{Im}_{\mathrm{res}}(i, j)$ is made taking into account the quality of pictures covering it, i.e., the mask of reconstructed pixels, since the result of classification of reconstructed pixels is not very reliable:

$$\mathrm{Im}_{\mathrm{res}}(i, j) = \begin{cases} \mathrm{Im}_1(i, j), & \mathrm{Mask}\,(\mathrm{Im}_1) < \mathrm{Mask}\,(\mathrm{Im}_2), \\ \mathrm{Im}_2(i, j), & \mathrm{Mask}\,(\mathrm{Im}_1) \ge \mathrm{Mask}\,(\mathrm{Im}_2), \end{cases}$$

where $\mathrm{Im}_1(i, j)$ and $\mathrm{Im}_2(i, j)$ are the results of classification of pixel (i, j), $\mathrm{Mask}\,(\mathrm{Im}_i)$ is the number of reconstructed pixels on the image whose classification result is Im_i, $i = \overline{1, 2}$.

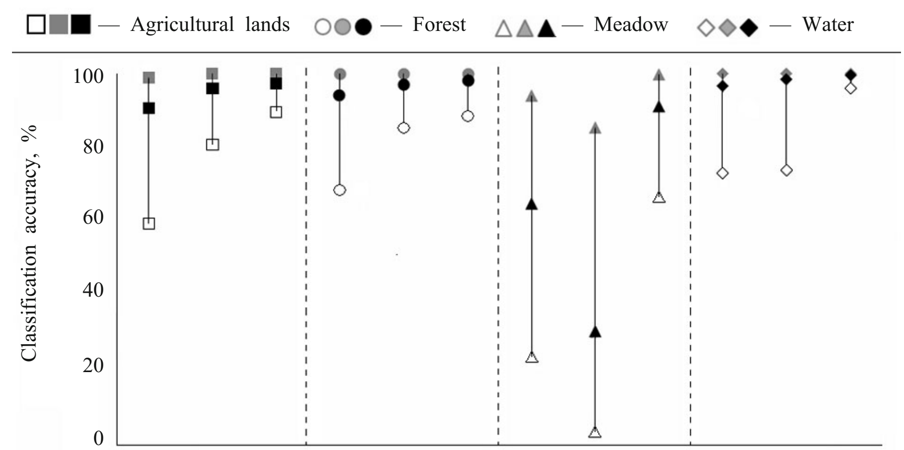

Max	98.8	100	99.9	99.8	100	100	94	85.3	99.7	100	100	100
Mean	90.65	95.97	97.25	94.08	97.04	98.13	64.82	30.58	91.06	96.55	98.24	99.53
Min	59.5	80.8	89.6	68.7	85.6	88.5	23.6	3.4	66.9	73.3	73.7	96.2

Fig. 5. Producer's accuracy scatter for three methods of data fusion in constructing classification maps for 2010.

ANALYSIS OF THE RESULTS

The proposed approach was used to create land cover maps for the territory of Ukraine based on the Landsat data for 1990, 2000, and 2010. The comparative analysis of the results of different methods of data fusion in constructing classification maps shows that the accuracy scatter of the user and the producer for the main classes of land cover (agricultural lands, forest, uncultivated land, and water) is rather large. Figures 5 and 6 show the minimum, medium, and maximum values of the accuracy of the producer and the user for four main classes of land cover when three methods of data fusion are used. Light symbols correspond to the minimum values of each class and gray to maximum ones. In the pictures, vertical dash and dotted lines separate the results for each class. In each section, corresponding to a certain class of land cover, the values of accuracy ensured by three different methods of data fusion are presented. From left to right, the figures show the results of fusion on the basis of probability, with regard for cloudiness mask and data fusion at pixel level (classification in time series of images). The two first results for each class (from left to right) correspond to fusion methods at decision-making level: on the basis of probability and with regard for cloud mask. The third result in each section corresponds to data fusion at pixel level (classification in time series of images).

In what follows, for brevity, we will call uncultivated lands meadows.

As is seen from Figs. 5 and 6, the method of data fusion at pixel level (classification in time series of pictures) ensures the best results for both user's and producer's accuracy. The greatest scatter in the results is observed in meadow classification. This is due to similarity of spectral characteristics of different types of vegetation (on agricultural and non-agricultural areas) and therefore, to the complexity of separating a meadow and agricultural crops.

Due to the advantage of the classification method based on time series, it was this method that was used to create resultant classification maps for 1990, 2000, and 2010. For each region, the overall classification accuracy is no less than 88% (97% on the average) on independent test sample. The minimum classification accuracy is observed in Dnipropetrovsk (in 1990) and Lviv (in 2010) regions. This is because of insufficient amount of satellite data in 1990 and noisiness (cloudiness) of the majority of pictures that cover Lviv region in 2010. The histogram of the general land cover classification accuracy for each region for 1990, 2000, and 2010 is given in Fig. 7.

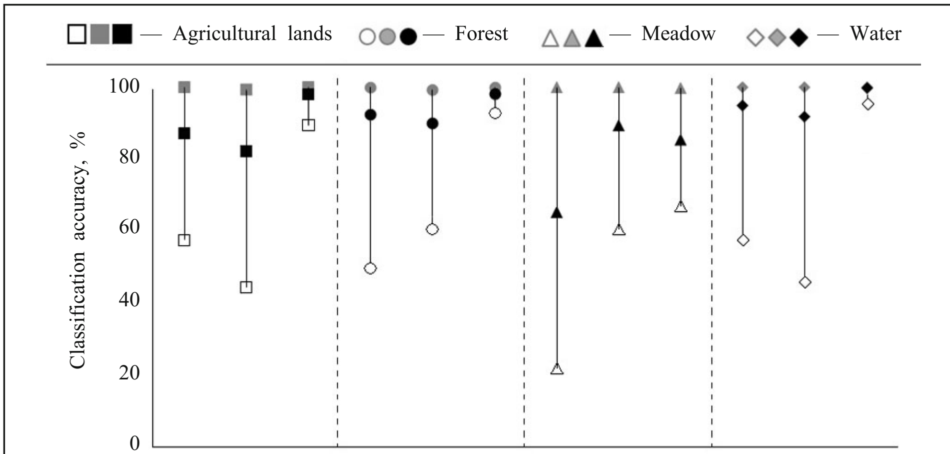

Max	99.9	99.4	100	99.9	99.4	99.9	99.9	100	99.8	100	100	100
Mean	87.28	82.12	98.08	92.42	89.94	98.24	65.41	89.28	85.43	95.0	91.76	99.64
Min	57.5	44.4	89.3	49.9	60.6	93.1	21.8	60.7	67	57.7	45.9	95.6

Fig. 6. User's accuracy scatter for three methods of data fusion in constructing classification maps for 2010.

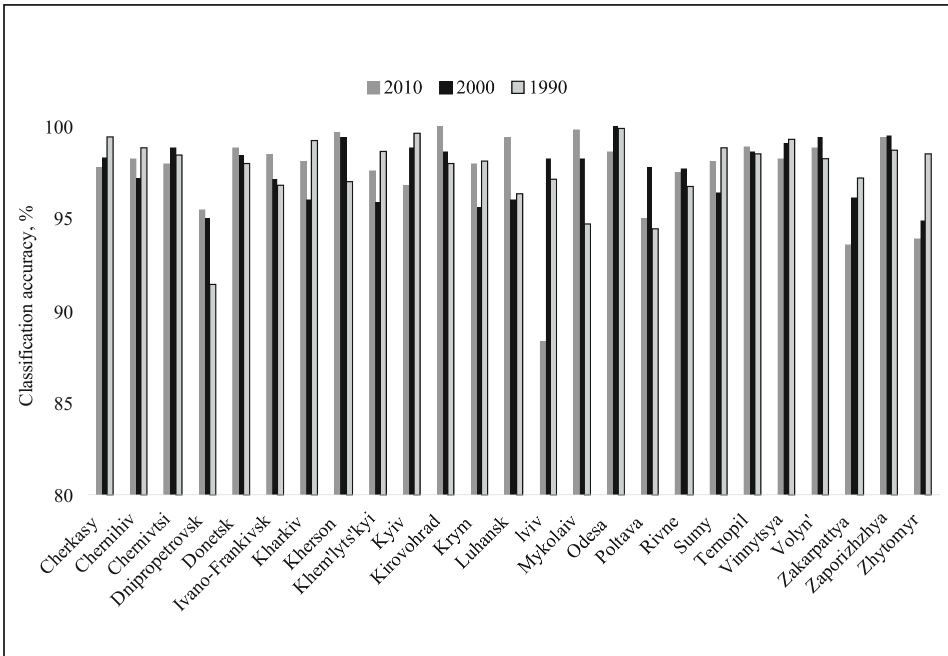

Fig. 7. Histogram of the general classification accuracy for each region.

The obtained land cover classification maps are of rather high accuracy. The accuracy scatter of the user and the producer in the main classes of land cover for 1990, 2000, and 2010 is presented in Figs. 8 and 9. As the studies have shown, the best classification results (the least accuracy scatter) are attained for forest and water. The greatest accuracy scatter in the construction of land cover map corresponds to the class of uncultivated land, whose minimum value is about 66%.

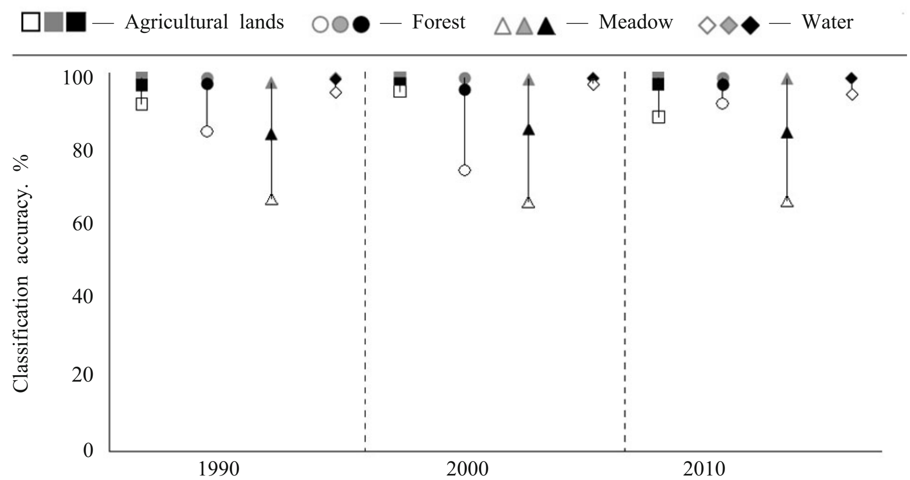

Max	99.9	99.9	98.7	100	100	99.9	99.5	100	100	99.9	99.8	100
Mean	98.07	98.33	84.83	99.6	98.43	96.95	86.24	99.82	98.08	98.24	85.43	99.64
Min	92.9	85.8	67.4	96.3	96.1	75.4	66.7	98.1	89.3	93.1	67	95.6

Fig. 8. User's accuracy scatter for the main classes in case of classification on the basis of time series of images.

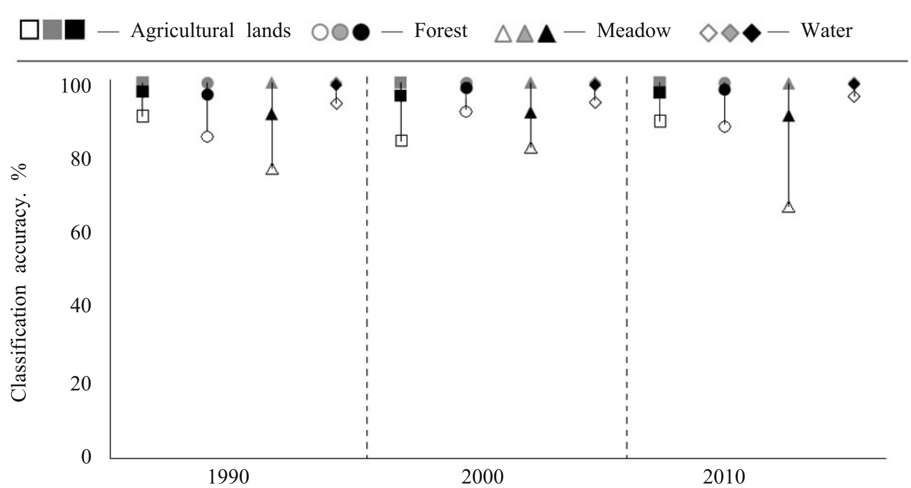

Max	100	100	99.8	100	100	100	99.8	100	99.9	100	99.7	100
Mean	97.52	96.76	91.61	99.16	96.42	98.66	92.03	99.15	97.25	98.13	91.06	99.53
Min	91	85.5	76.9	94.4	84.3	92.5	82.7	94.6	89.6	88.5	66.9	96.2

Fig. 9. Producer's accuracy scatter for the main classes in case of classification on the basis of time series of images.

CONCLUSIONS

In the present paper, we have considered the problem of large-scale land cover mapping on the basis of retrospective data of high resolution as a problem of automated handling of bid geospatial data that may contain uncertainties (for example, areas hidden by clouds). To solve the problem, we have proposed to use three paradigms of computer sciences, namely, the decomposition technique ("divide and conquer") from the theory of algorithms, the method of active training from intelligent computing, and the method of reconstruction of satellite pictures from computer processing of digital images. Complex application of these three components allows us to minimize the involvement of an expert in problem solution. We have analyzed three variants of data fusion in the land cover classification problem: two variants at decision making level and one at pixel level. We have shown the efficiency of the last data fusion method, which reduces to solving the classification problem based on data time series. Due to the developed automated methodology, it became possible for the first time to solve the problem of classification and mapping of land cover of the whole territory of Ukraine for 1990, 2000, and 2010 with a 30-meter resolution. The total accuracy of classification by fields is no less than 88% and is 97% on the average on an independent test sample.

The results obtained in solving the mapping problem can be used for risk assessment and to solve other important applied problems [25, 26].

REFERENCES

1. M. A. Friedl, D. K. McIver, J. C. F. Hodges, X. Y. Zhang, D. Muchoney, A. H. Strahler, C. E. Woodcock, S. Gopal, A. Schneider, A. Cooper, A. Baccini, F. Gao, and C. Schaaf, “Global land cover mapping from MODIS: Algorithms and early results,” Remote Sensing of Environment, **83**, No. 2, 287–302 (2002).
2. J. Gallego, N. Kussul., S. Skakun, O. Kravchenko, A. Shelestov, and O. Kussul, “Efficiency assessment of using satellite data for crop area estimation in Ukraine,” Intern. J. Applied Earth Observation and Geoinformation, **29**, 22–30 (2014).
3. N. Kussul, S. Skakun, A. Shelestov, O. Kravchenko, J. F. Gallego, and O. Kussul, “Crop area estimation in Ukraine using satellite data within the MARS project 2012,” IEEE Intern. Geoscience and Remote Sensing Symposium (IGARSS) (2012), pp. 3756–3759.
4. T. H. Cormen, C. E. Leiserson, R. L. Rivest, and C. Stein, Introduction to Algorithms, The MIT Press, Cambridge, MA (2009).
5. D. Tuia, F. Ratle, F. Pacifici, M. F. Kanevski, and W. J. Emery, “Active learning methods for remote sensing image classification,” IEEE Trans. on Geoscience and Remote Sensing, **47**, No. 7, 2218–2232 (2009).
6. A. Yu. Shelestov, A. N. Kravchenko, S. V. Skakun, S. V. Voloshin, and N. N. Kussul, “Geospatial information system for agricultural monitoring,” Cybern. Syst. Analysis, **49**, No. 1, 124–132 (2013).
7. N. Kussul, S. Skakun, A. Shelestov, O. Kussul, and B. Yailymov, “Resilience aspects in the sensor Web infrastructure for natural disaster monitoring and risk assessment based on Earth observation data,” IEEE J. Selected Topics in Applied Earth Observations and Remote Sensing, **7**, No. 9, 3826–3832 (2014).
8. N. Kussul, D. Mandl, K. Moe, J. P. Mund, J. Post, A. Shelestov, S. Skakun, J. Szarzynski, G. Van Langenhove, and M. Handy, “Interoperable infrastructure for flood monitoring: Sensor Web, Grid, and cloud,” IEEE J. Selected Topics in Applied Earth Observations and Remote Sensing, **5**, No. 6, 1740–1745 (2012).
9. N. Kussul, A. Shelestov, and S. Skakun, “Grid and sensor Web technologies for environmental monitoring,” Earth Science Informatics, **2**, No. 1–2, 37–51 (2009).
10. N. Kussul, A. Shelestov, and S. Skakun, “Flood monitoring from SAR data,” NATO Science for Peace and Security Series C: Environmental Security, 19–29, 10.1007/978-90-481-9618-0_3 (2011).
11. S. V. Skakun and R. M. Basarab, “Reconstruction of missing data in time-series of optical satellite images using self-organizing Kohonen maps,” J. Autom. Inform. Sci., **46**, No. 12, 19–26 (2014).
12. M. C. Hansen, A. Egorov, D. P. Roy, P. Potapov, J. Ju, S. Turubanova, I. Kommareddy, and T. R. Loveland, “Continuous fields of land cover for the conterminous United States using Landsat data: First results from the Web-Enabled Landsat Data (WELD) project,” Remote Sensing Letters, **2**, No. 4, 279–288 (2011).
13. G. Büttner, J. Feranec, G. Jaffrain, L. Mari, G. Maucha, and T. Soukup, “The CORINE land cover 2000 project,” EARSeL eProceedings, **3**, No. 3, 331–346 (2004).
14. N. Kussul, S. Skakun, A. Shelestov, and O. Kussul, “The use of satellite SAR imagery to crop classification in Ukraine within JECAM project,” in: IEEE Intern. Geoscience and Remote Sensing Symposium (IGARSS) (2014), pp. 1497–1500.

15. N. Kussul, S. Skakun, A. Shelestov, O. Kravchenko, and O. Kussul, “Crop classification in Ukraine using satellite optical and SAR images,” Models&Analyses, **2**, No. 2, 118–128 (2013).
16. J. Gallego, A. N. Kravchenko, N. N. Kussul, S. V. Skakun, A. Yu. Shelestov, Yu. A. Grypych, “Efficiency assessment of different approaches to crop classification based on satellite and ground observations,” J. Autom. Inform. Sci., **44**, No. 5, 67–80 (2012).
17. Chen Jun, Chen Jin, A. Liao, X. Cao, L. Chen, X. Chen, He C., G. Han, S. Peng, M. Lu, W. Zhang, X. Tong, and J. Mills, “Global land cover mapping at 30m resolution: A POK-based operational approach,” ISPRS J. of Photogrammetry and Remote Sensing, **103**, 7–27 (2015).
18. S. Haykin, Neural Networks and Learning Machines, Prentice Hall, Upper Saddle River (NJ) (2008).
19. J. Sim and C. C. Wright, “The Kappa statistic in reliability studies: Use, interpretation, and sample size requirements,” Physical Therapy, **85**, No. 3, 257–268 (2005).
20. LUCAS, Land use and cover area frame survey (2009), http://ec.europa.eu/eurostat/documents/205002/208938/LUCAS2009_C1-Instructions_Revised20130925.pdf/.
21. P. Olofsson, G. M. Foody, M. Herold, S. V. Stehman, C. E. Woodcock, and M. A. Wulder, “Good practices for estimating area and assessing accuracy of land change,” Remote Sensing of Environment, **148**, 42–57 (2014).
22. G. M. Foody, “Status of land cover classification accuracy assessment,” Remote Sensing of Environment, **80**, No. 1, 185–201 (2002).
23. N. Kussul, S. Skakun, A. Shelestov, and O. Kussul, “The use of satellite SAR imagery to crop classification in Ukraine within JECAM project,” Geoscience and Remote Sensing Symposium (IGARSS), IEEE Intern., Quebec City, QC, Canada (2014), pp. 1497–1500, DOI: 10.1109/IGARSS.2014.6946721.
24. V. Lavreniuk, N. Kussul, S. Skakun, A. Shelestov, and B. Yailymov, “Regional retrospective high resolution land cover for Ukraine: Methodology and results,” Intern. Geoscience and Remote Sensing Symposium (IGARSS) (2015).
25. N. N. Kussul, B. V. Sokolov, Ya. I. Zyelyk, S. V. Skakun, and A. Yu. Shelestov, “Disaster risk assessment based on heterogeneous geospatial information,” J. Autom. Inform. Sci., **42**, No. 12, 32–45 (2010).
26. S. Skakun, N. Kussul, A. Shelestov, and O. Kussul, “Flood hazard and flood risk assessment using a time series of satellite images: A case study in Namibia,” Risk Analysis, **34**, No. 8, 1521–1537 (2014).